MATEMATIKA: MJIAM, 2019, Volume 35, Number 2, 260–270

g-Jitter Free Convection Flow of Nanofluid in The Three-Dimensional Stagnation Point Region

Mohamad Hidayad Ahmad Kamal*, **Anati Ali and Sharidan Shafie**
Department of Mathematical Sciences, Universiti Teknologi Malaysia
81310 UTM Johor Bahru, Malaysia
*Corresponding author: mohamadhidayadahmadkamal@gmail.com

Article history
Received: 8 October 2018
Received in revised form: 18 April 2019
Accepted: 19 April 2019
Published online: 1 August 2019

Abstract The three dimensional free convection boundary layer flow near a stagnation point region is embedded in viscous nanofluid with the effect of g-jitter is studied in this paper. Copper (Cu) and aluminium oxide (Al_2O_3) types of water base nanofluid are chosen with the constant Prandtl number, Pr=6.2. Based on Tiwari-Das nanofluid model, the boundary layer equation used is converted into a non-dimensional form by adopting non-dimensional variables and is solved numerically by engaging an implicit finite-difference scheme known as Keller-box method. Behaviors of fluid flow such as skin friction and Nusset number are studied by the controlled parameters including oscillation frequency, amplitude of gravity modulation and nanoparticles volume fraction. The reduced skin friction and Nusset number are presented graphically and discussed for different values of principal curvatures ratio at the nodal point. The numerical results shows that, increment occurs in the values of Nusset number with the presence of solid nanoparticles together with the values of the skin friction. It is worth mentioning that for the plane stagnation point there is an absence of reduced skin friction along the y-direction where as for axisymmetric stagnation point, the reduced skin friction for both directions are the same. As nanoparticles volume fraction increased, the skin friction increased as well as the Nusset number. The results, indicated that skin frictions of copper are found higher than aluminium oxide.

Keywords g-Jitter; stagnation point; three-dimensional body; nanofluids.

Mathematics Subject Classification 35Q06, 76D06.

1 Introduction

In fluid mechanics discipline, stagnation point is defined as a point where the local velocity of the fluid flow is equal to zero [1]. Encounter of fluid with any shapes of boundary layer geometry generate a stagnation points flow cases which exist at the surface of an object and the velocity of flow field is brought to rest by the object. Lok [2] has mentioned that for the two dimensional plane stagnation point flow, Heimenz in [3] was the first in interpreting the problem into Navier-Stokes equation and being analyses in term of the velocity distribution. In 1936, Homann was the first in conducting a theoretical study for stagnation point flow for a flat surface geometry which then correspond to the axisymmetric case stagnation point flow [4]. The research was then extended by [4] as well as other researchers in exploring effects including the wall stretching, suction and blowing through a porous medium.

Lok [5] investigated the viscous and incompressible fluid behavior near the two-dimensional stagnation point flow cases with fluid impinging on the stretching sheet at the boundary. The research then continued by Lapropulu [6] by using non-Newtonian fluid which is Walters' B' fluid with chosen geometry of infinite plate which normal to the flow induced with magnetic field effect. From the investigations, it was found that the Hartmanns number give a significant effect to the velocity of the fluid near the wall with the increment of Hartmanns number increased the speed of the fluid. On the other hand, [7] examined the studies by assuming that the fluid flow at the free stream is on the same direction of magnetic fiend for plane orthogonal stagnation-point in steady case flow.

In 1951, Howarth [8] generalized the nonlinear interaction bounded by two orthogonal Hiemanz flows into three-dimensional stagnation point flow with the companionship of arbitrary strain rate. Later, with the same mathematical model problem formulation, a study was conducted [9] by changing the geometry of boundary layer into permeable moving surface together with anisotropic slip condition for steady laminar viscous fluid. Again, some researches are conducted in making the changes of boundary layer geometry when [10] investigated the effect of stagnation point flow on heat transfer for three dimensional steady laminar flow cases with stretched exponentially surface of boundary layer. The modification on mathematical formulation of Homann stagnation point flow was then done by Mahapatra [11] when the axisymmetric flow changed into non-axisymmetric stagnation point flow towards a rigid stretching sheet plate.

On the other hand, microgravity environment is found to be one of the factors in increasing the final product material based on crystal growth. An experiment study was conducted in analyzing crystal growth at outer space and it was found that it still faces small fluctuating gravitational field distribution which then known as g-jitter. Fluid flow induced by g-jitter is found affected on its convection when the interaction of density gradient is different compared to the normal gravity field correspond to fluid motion behavior. Theoretical study on the boundary layer flow induced by g-jitter has being conducted by Rees and Pop [12] for the flow of forward stagnation point with cylindrical shape of boundary layer embedded in porous medium fluid. A study on mixed convection of mass and heat transfer was then conducted by Sharidan [13] while considering a system of two heated vertical parallel infinite plates with different concentration and temperature while the temperature remained unchanged and g-jitter effect are considered. The same researcher extent his study by considering g-jitter in [14] for a three-dimensional stagnation point flow problem with free convection flow.

Rigorous studies of nanofluid have conducted many theoretical and experimental investigations in escalation of the heat transfer enhancement. The nanofluid study implicate to stagnation point boundary layer flow has being conducted by Babu and Sandeep [15]. A stretching sheet boundary and non linear thermal radiation is studied by adding nanoparticles dwell of gyrotactic microorganisms with the presence of non align magnetic field. Another study was conducted in [16] by solving and analyzing heat transfer properties for two-dimensional stagnation point problem in non Newtonian nanofluid with the presence of thermal radiation and chemical reaction through inclined stretching sheet boundary. As for the steady case problem, Amirson [17] conducted a study to analyze the multi properties nanofluid on the three-dimensional stagnation point flow with zero mass flux boundary condition.

Motivate from the previous researches, a numerical study was done on a boundary layer incompressible viscous nanofluid flow near a three-dimensional stagnation point induced by g-jitter. This research was an extension from a study conducted by Sharidan [18] by adding a small amount of nanoparticles on the conventional fluid. The problem was govern mathematically and solved numerically using implicit finite difference procedure known as Keller box method. The result of physical quantities of principal interest such as skin friction on both directions and Nusset number are analyzed based on the parameter involved such as amplitude of modulation, curvature ratio, frequency of oscillation and nanoparticles volume fraction.

2 Mathematical Formulation

Consider a free convection flow induced by g-jitter on a three-dimensional stagnation point region which the body of the boundary is heated in incompressible viscous water-based nanofluid. Copper (Cu) and aluminum oxide (Al_2O_3) nanoparticles were chosen and the problem was govern based on nanofluid model proposed by Tiwari and Das [19]. The temperature of the body was assumed was T_w while T_∞ is the initial temperature of the fluid in which the temperature for both were assumed to be consistent. The flow on a stagnation point region was found to be wavy due to the result of a flow that hit the surface which locate the exact stagnation point. As a result, the wavy flow produced two important points that indicated the flow near a stagnation point region known as Nodal point, **N** and saddle point, **S**. Nodal point is chosen to represent the stagnation point case flow which then transformed into Cartesian orthogonal system (x, y, z) where **N** is at the origin for the capacity of nodal point as shown in Figure 1.The $x-$ and $y-$coordinates are measured along the body surface, while the $z-$coordinate is measured normal to the body surface.

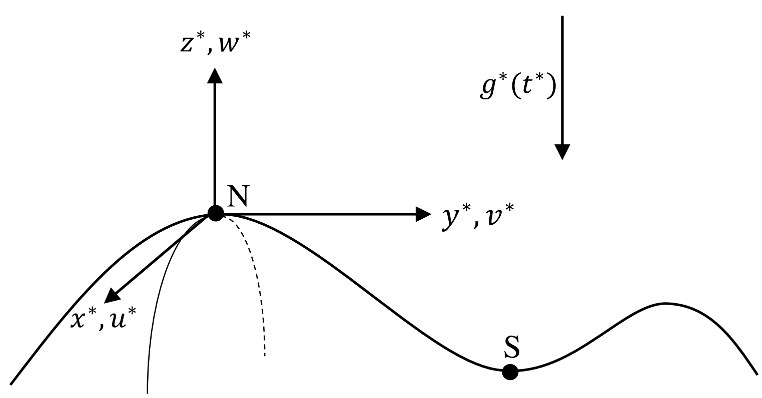

Figure 1: Physical Model Representation of Stagnation Point Region in Cartesian Coordinate System

g-Jitter induced to the problem lead to the gravitational field which depends on time takes the form as

$$g^*(t^*) = g_0[1 + \varepsilon \cos(\pi\omega t)] \tag{1}$$

where g_0 indicated the mean of gravitational acceleration, ε is the scaling parameter representing the amplitude of gravity modulation, ω is the frequency of oscillation for the flow induced by g-jitter and t is the time. By applying boundary layer and Boussinesq approximation which also supported by the literature, the boundary layer governing equations that represent the three dimensional stagnation point free convection flow induced by g-jitter are

$$\frac{\partial u^*}{\partial x^*}+\frac{\partial v^*}{\partial y^*}+\frac{\partial w^*}{\partial z^*}=0 \tag{2}$$

$$\rho_{nf}\left(\frac{\partial u^*}{\partial t^*}+u^*\frac{\partial u^*}{\partial x^*}+v^*\frac{\partial u^*}{\partial y^*}+w^*\frac{\partial u^*}{\partial z^*}\right)=\mu_{nf}\frac{\partial^2 u^*}{\partial z^{*2}}+g^*(t^*)(\rho\beta)_{nf}ax^*(T-T_\infty) \tag{3}$$

$$\rho_{nf}\left(\frac{\partial v^*}{\partial t^*}+u^*\frac{\partial v^*}{\partial x^*}+v^*\frac{\partial v^*}{\partial y^*}+w^*\frac{\partial v^*}{\partial z^*}\right)=\mu_{nf}\frac{\partial^2 v^*}{\partial z^{*2}}+g^*(t^*)(\rho\beta)_{nf}by^*(T-T_\infty) \tag{4}$$

$$\frac{\partial T}{\partial t^*}+u^*\frac{\partial T}{\partial x^*}+v^*\frac{\partial T}{\partial y^*}+w^*\frac{\partial T}{\partial z^*}=\alpha_{nf}\frac{\partial^2 T}{\partial z^{*2}} \tag{5}$$

subject to initial and boundary conditions

$$\begin{aligned}
t^*<0: & u^*=v^*=w^*=0,\quad T=T_\infty \quad \text{for any} \quad x^*,y^* \quad \text{and} \quad z^*\\
t^*\geq 0: & u^*=v^*=0,\quad T=T_w \quad \text{on} \quad z^*=0,\quad x^*\geq 0,\quad y^*\geq 0\\
& u^*=v^*=0,\quad T=T_\infty,\quad \text{on} \quad x^*=0,\quad y^*\geq 0,\quad z^*>0\\
& u^*=v^*=0,\quad T=T_\infty,\quad \text{on} \quad y^*=0,\quad x^*\geq 0,\quad z^*>0\\
& u^*=v^*=0,\quad T=T_\infty,\quad \text{as} \quad z^*\to\infty,\quad x^*\geq 0,\quad y^*>0
\end{aligned} \tag{6}$$

where u^*, v^*, w^* represent the three components of velocity along the x^*, y^*, z^* axes, T indicates the fluid temperature and $\rho_{nf}, \mu_{nf}, \beta_{nf}, \alpha_{nf}$ represent all the parameters involving nanonofluid which are the density, dynamic viscosity, thermal expansion and thermal diffusion with subscript nf is nanofluid. The stagnation point parameter indicated by constant a and b are the principal curvatures at the nodal point which measured from xy plane. The chosen value for b indicated the outcome of the stagnation point flow cases such as plane stagnation point flow happen when $b=0$ and $b=a$ resemble the axisymmetric stagnation point flow case. In studying the stagnation point at the nodal point, the chosen values for a and b need to be larger than zero correspond to $c=\frac{b}{a}$. Practically, most of the shape lies between cylinder and sphere geometry where the curvature ratio values c, is between 0 and 1. The negative value of a and b will lead to saddle point $\mathbf{S}$, at the stagnation-point. From [20], the nanofluid constants are then defined as;

$$\begin{aligned}
\mu_{nf}&=\frac{\mu_f}{(1-\phi)^{2.5}}, & \alpha_{nf}&=\frac{k_{nf}}{(\rho C_p)_{nf}},\\
\rho_{nf}&=(1-\phi)\,\rho_f+\phi\rho_s, & (\rho\beta)_{nf}&=(1-\phi)\,(\rho\beta)_f+\phi(\rho\beta)_s,\\
(\rho C_p)_{nf}&=(1-\phi)\,(\rho C_p)_f+\phi(\rho C_p)_s, & \frac{k_{nf}}{k_f}&=\frac{(k_s-2k_f)-2\phi\,(k_f-k_s)}{(k_s-2k_f)+\phi\,(k_f-k_s)},
\end{aligned} \tag{7}$$

where ϕ represented the nanofluid parameter known as nanoparticle volume fraction, k hold the thermal conductivity parameter, C_p served as the specific heat at constant pressure and the

Table 1: Thermophysical Properties of Nanoparticles and Base Fluid

Physical Properties	Water	Copper	Aluminium
$\rho(\text{kgm}^{-3})$	997.1	8933	3970
$C_p(\text{Jkg}^{-1}\text{K}^{-1})$	4179	385	765
$k(\text{Wm}^{-1}\text{K}^{-1})$	0.613	401	40
$\beta \times 10^5(\text{K}^{-1})$	5.21	1.67	0.85

subscript f and s are for fluid and solid. The information for chosen nanoparticles and base fluid are shown in term of thermophysical properties as illustrated in Table 1.

The complexity of the problem is reduced using similarity transformation technique. Equations (2) – (5) together with the initial and boundary conditions (6) will permit a semi-similar solution [18],

$$\begin{aligned} \eta &= Gr^{1/4}az^*, & t &= \nu a^2 Gr^{1/2}t^*, & u^* &= \nu a^2 x^* Gr^{1/2} f'(t,\eta) \\ v^* &= \nu a^2 y^* Gr^{1/2} h'(t,\eta), & \tau &= \Omega t, & w^* &= -\nu a Gr^{1/4}(f+h) \\ \theta(t,\eta) &= \frac{(T-T_\infty)}{(T_w-T_\infty)}, & \Omega &= \frac{\omega}{\nu a^2 Gr^{1/2}}, & g(t) &= \frac{g^*(t^*)}{g_0} \end{aligned} \tag{8}$$

where Grashof number is denoted as $Gr = g_0\beta(T_w - T_\infty)/(a^3\nu^2)$ and primes notation at the partial differential are respected to η. By substituting equations (7) and (8) into (2)–(5), the following governing equation is produced,

$$C_1 f''' + C_2[(f+h)f'' - f'^2] + C_3[1+\varepsilon\cos(\pi\tau)]\theta = C_2\Omega\frac{\partial f'}{\partial \tau} \tag{9}$$

$$C_1 h''' + C_2[(f+h)h'' - h'^2] + C_3 c[1+\varepsilon\cos(\pi\tau)]\theta = C_2\Omega\frac{\partial h'}{\partial \tau} \tag{10}$$

$$\frac{C_4}{\text{Pr}}\theta'' + (f+h)\theta' = \Omega\frac{\partial \theta}{\partial \tau} \tag{11}$$

where

$$\begin{aligned} C_1 &= \frac{1}{(1-\phi)^{2.5}}, \\ C_2 &= \left(1-\phi+\frac{\phi\rho_s}{\rho_f}\right), \\ C_3 &= \left(1-\phi+\frac{\phi\rho\beta_s}{\rho\beta_f}\right), \\ C_4 &= \frac{k_{nf}/k_f}{\left[1-\phi+\frac{\phi(\rho C_p)_s}{(\rho C_p)_f}\right]}, \end{aligned} \tag{12}$$

with the boundary conditions (6) become

$$\begin{gathered} f(\tau,0)=f'(\tau,0)=0, \qquad h(\tau,0)=h'(\tau,0)=0, \qquad \theta(\tau,0)=1, \\ f'\to 0 \qquad h'\to 0 \qquad \theta\to 0 \qquad \text{as} \;\; \eta\to\infty, \end{gathered} \tag{13}$$

The fluid flow behavior is analyzed in term of skin friction coefficients in $x-$ and $y-$directions, C_{fx} and C_{fy} together with the Nusselt number, Nu which measured normal to the xy plane which designate as,

$$\begin{aligned} C_{fx} &= \mu_{nf}\left(\frac{\partial u^*}{\partial z^*}\right)_{z^*=0} \Big/ \left(\rho_{nf}{\nu_{nf}}^2 a^3 x^*\right), \\ C_{fy} &= \mu_{nf}\left(\frac{\partial v^*}{\partial z^*}\right)_{z^*=0} \Big/ \left(\rho_{nf}{\nu_{nf}}^2 a^3 y^*\right) \\ Nu &= -a^{-1}k_{nf}\left(\frac{\partial T}{\partial z^*}\right)_{z^*=0} \Big/ k_f\left(T_w - T_\infty\right) \end{aligned} \tag{14}$$

,

where μ_{nf} is the dynamics viscosity of the nanofluid. In terms of non-dimensional variables, we have

$$\begin{aligned} C_{fx}/Gr^{3/4} &= f''(\tau,0)/(1-\phi)^{2.5}, \\ C_{fy}/Gr^{3/4} &= h''(\tau,0)/(1-\phi)^{2.5}, \\ Nu/Gr^{1/4} &= -(k_{nf}/k_f)\theta'(\tau,0). \end{aligned} \tag{15}$$

3 Methodology

The non-dimensional partial differential equations (9)–(11) and non-dimensional boundary conditions (13) will be solved using implicit finite different procedure which already discussed in detail by Cebeci and Bradshaw [17] known as Keller box method. There are a few steps to solve the partial differential equation using Keller box method which is the first and foremost in ensuring the equation is on first order system. Some modifications on the partial differential equation will be conducted in reducing the order of the system and finite central different method will discretize the system of equation later. The resulting product on the coefficient matrix from the discretization procedure is then linearize using Newton's method. The final product of linear system of equation is then solved by employing block triadiagonal elimination method.

The present study analyses the behavior of skin frictions on both directions and the Nusset number while considering controlling parameters such as curvature ratio at the stagnation-point c, oscillation frequency Ω and amplitude of gravity modulation ε. Since we are considering nanofluid, the nanofluid parameter such as volume fraction of nanoparticle ϕ and types of nanoparticle are also considered. Two types of nanoparticle were chosen which are copper (Cu) and aluminum oxide (Al_2O_3) while water based fluid are considered correspond to Prandtl number Pr=6.2.

All the result were collected using same size of grids in both τ and η direction with $\Delta\tau = 0.1$ and $\Delta\eta = 0.04$. The iteration will be stopped when it reached the stopping criteria, the maximum absolute point change between iteration is less than 10^{-10} and the solution are considered converged. On each specific parameter which represent the effect on the flow, the selected range are $0 \leq \varepsilon \leq 1$ for the amplitude of modulation, $\Omega = 0.2$ and 5 are selected to study the different size of frequency of single-harmonic oscillation and the curvature ratio $c = 0, 0.5, 1$ to study the effect of the stagnation point flow. From the literature and conducted study in this paper, the gravitational field is found to reverse its direction due to the g-jitter effect for the amplitude of modulation $\varepsilon > 1$. The result is then presented graphically correspond to the effect for each parameter and discussed briefly in the next sub chapter.

4 Result and Discussion

Keller box method was used to solve the non-dimensional partial differential equations (9)–(11) together with its boundary condition in (13) numerically. Skin frictions for both directions and the Nusset number are chosen in analyzing physical quantities of principal interest of the flow at a stagnation point region by considering effect such as g-jitter and nanofluid. A comparison was made with previous study conducted by Sharidan [18] when nanofluid is not considered in their problem with parameter values chosen were $\phi = 0, Pr = 0.72, c = 0.5$ and $\Omega = 0.2$ with various values of ε as shown in Table 2. The comparison result in Table 2 in term of skin frictions and Nusset number showed very good agreement with previous studies.

Table 2: Comparison results of the skin friction and rate of heat transfer with $c = 0.5$, $\Omega = 0.2$, $\mathrm{Pr} = 0.72$ with different values of ε.

ε	Sharidan [18]			Present		
	f''	h''	θ'	f''	h''	θ'
0.0	0.7991	0.4266	0.4287	0.7989	0.4264	0.4287
0.2	0.7976	0.4260	0.4280	0.7980	0.4260	0.4280
0.4	0.7940	0.4240	0.4258	0.7946	0.4243	0.4258
0.6	0.7875	0.4207	0.4219	0.7885	0.4212	0.4219
0.8	0.7780	0.4161	0.4160	0.7794	0.4167	0.4160
1.0	0.7652	0.4100	0.4071	0.7669	0.4108	0.4071

Figure 2 shows the skin friction on $x-$ and $y-$directions together with Nusset number for $c = 0$, $\phi = 0.05$, $\Omega = 0.2$, $\mathrm{Pr} = 6.2$ with different values of amplitude of gravity modulation ε. It can be seen clearly that with the increased of ε, the variation of skin friction and Nusset number are almost proportional increase and decrease. Interestingly, the skin friction on $y-$direction showed no significant changes as the values of ε increases. A special type of stagnation case flow is identified when $c = 0$ which is plane stagnation case flow caused by cylindrical surface.

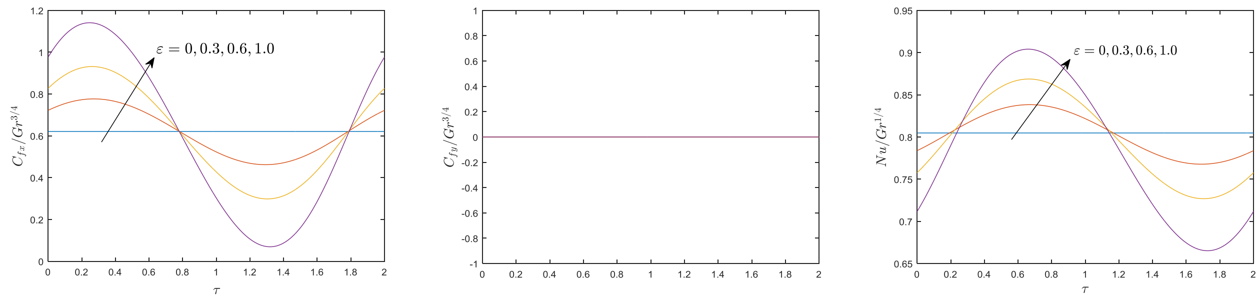

Figure 2: Skin Frictions and Nusset Number for $c = 0$, $\phi = 0.05$, $\Omega = 0.2$, $\Pr = 6.2$ and Different Values of ε.

Different values of c parameter were than analyses in Figure 3 with $c = 0.5$, $\phi = 0.05$, $\Omega = 0.2$, $\Pr = 6.2$ as values of ε increases. The same behavior is found on the skin friction for both direction and Nusset number as the various of ε are increases. The fluctuating results on skin friction and Nusset number showed that there are singularity solution happen on the flow caused by g-jitter effect considered in this problem.

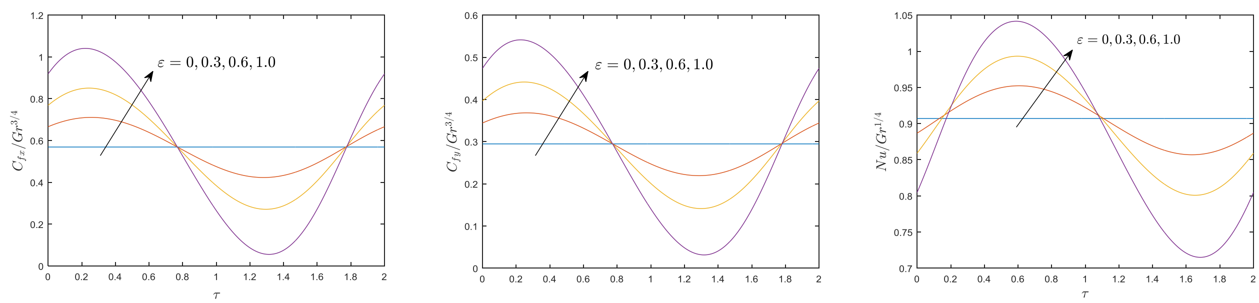

Figure 3: Skin Frictions and Nusset Number for $c = 0.5$, $\phi = 0.05$, $\Omega = 0.2$, $\Pr = 6.2$ and Different Values of ε.

The effect of amplitude gravity modulation parameter was also studied with constant $c = 1$, $\phi = 0.05$, $\Omega = 0.2$ and $\Pr = 6.2$ as illustrated in Figure 4. The skin friction and Nusset number are found increase and decrease with the increases of ε values. It is also found that the values of skin friction on both $x-$ and $y-$direction are the same which correspond to axisymmetric stagnation case flow. Axisymmetric stagnation case flow happen when the flow at stagnation point hit a cylindrical surface which is when $c = 1$.

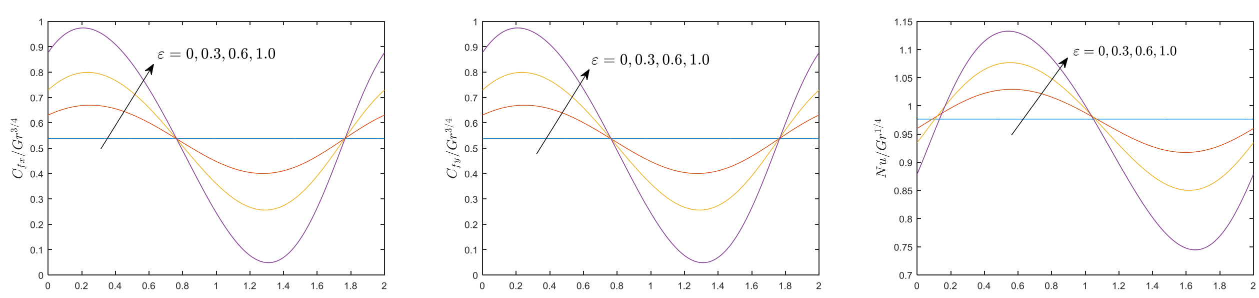

Figure 4: Skin Frictions and Nusset Number for $c = 1.0$, $\phi = 0.05$, $\Omega = 0.2$, $\Pr = 6.2$ and Different Values of ε.

Figure 5 illustrates the behavior of skin frictions and Nusset number under the effect of oscillation frequency parameter and amplitude of gravity modulation with constant values of

$c = 0.5$, $\phi = 0.05$ and $\Pr = 6.2$. Two values of oscillation frequency were chosen which are 0.2 and 5 to represent the different frequency period size. From the figure, both skin frictions Nusset number are found to be converging faster with bigger values of Ω. A smaller peak values of skin frictions are also found with bigger Ω and more significantly on Nusset number.

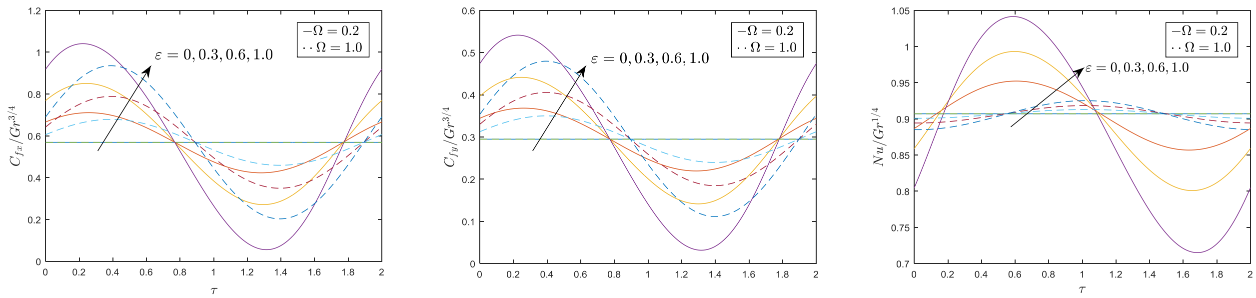

Figure 5: Skin Frictions and Nusset Number for $c = 0.5$, $\phi = 0.05$, $\Pr = 6.2$ and Different Values of ε and $\Omega = 0.2$.

Figure 6 shows the skin friction for both directions together with Nusset number with the constant value of $c = 0.5$, $\varepsilon = 0.5$, $\Omega = 0.2$ and $\Pr = 6.2$ parameter but different value of nanoparticle volume fraction ϕ which varies from $0 \leq \phi \leq 0.2$. The increasing of ϕ values produced increasing values of skin frictions on both directions and Nusset number. The increased values of skin frictions are due to the additional resistance contributed from nanoparticles. The enhancement of conventional fluid is also proven on Nusset number result by comparing the presence of nanoparticles on the fluid.

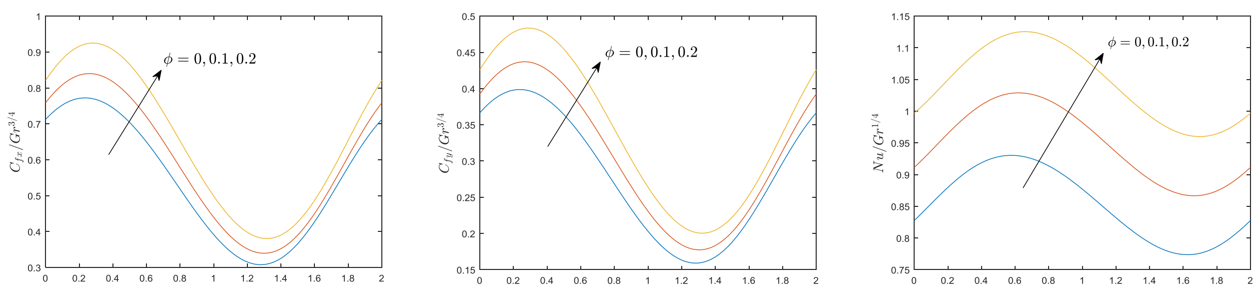

Figure 6: Skin Frictions and Nusset Number for $c = 0.5$, $\varepsilon = 0.5$, $\Omega = 0.2$ and $\Pr = 6.2$ with Different Values of ϕ.

Figure 7 illustrates the reduced skin friction for both directions and Nusset number on two different types of nanoparticles which are copper and aluminum oxide with constant values of $c = 0.5$, $\varepsilon = 0.5$, $\Omega = 0.2$ and $\Pr = 6.2$ with different values of ϕ. The result presented in graph shows that the skin frictions for copper are higher than aluminum oxide in both direction while the Nusset number for both nanoparticles are almost the same. The different results on skin frictions and Nusset number are due to the different thermophysical properties values carried by each type nanoparticles.

5 Conclusion

The three-dimensional free convection boundary layer flow near a stagnation point region embedded in viscous nanofluid with the effect of g-jitter has been solved using Keller box method

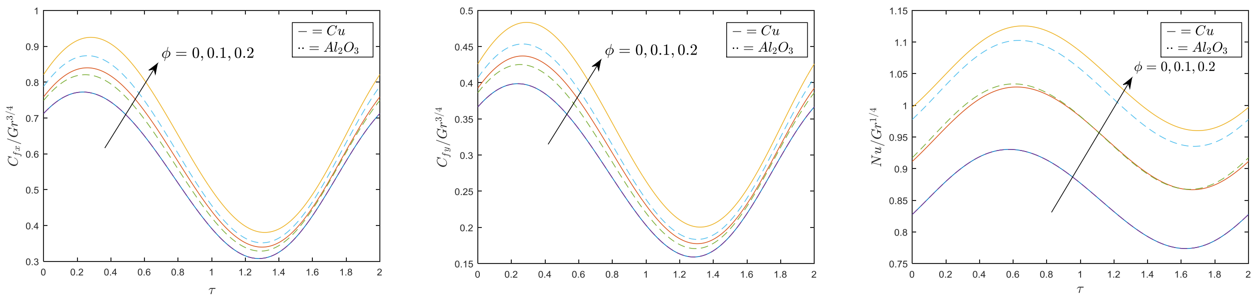

Figure 7: Skin Frictions and Nusset Number for $c = 0.5$, $\varepsilon = 0.5$, $\Omega = 0.2$ and $\mathrm{Pr} = 6.2$ with Different Values of ϕ and Types of Nanoparticles.

by considering constant wall temperature type of boundary condition. Copper (Cu) and aluminum oxide (Al_2O_3) nanoparticles with water-based nanofluid were chosen to analyze the effect of nanofluids on the boundary layer flow. The physical properties of principal interest analysis result in terms of skin frictions and rate of heat transfer coefficient by considering the effect of curvature ratio parameter in the nanofluid induced by g-jitter were presented graphically and discussed briefly in the previous section. The present results has been verified for the case of viscous fluid $\phi = 0$ reported by Sharidan [18] by controlling the amplitude of modulation parameter value.

Acknowledgments

The authors would like to acknowledge Ministry of Higher Education (MOHE) and Research Management Centre-UTM, Universiti Teknologi Malaysia (UTM) for the financial support through vote numbers 5F004 for this research.

References

[1] Clancy, L. J. *Aerodynamics*. London: Pitman Publishing Limited. 1975.

[2] Yian, L. Y. Mathematical Modelling of a Micropolar Fluid Boundary Layer Near a Stagnation-Point. Universiti Teknologi Malaysia: Ph.D. Thesis. 2008.

[3] Hiemenz, K. Die Grenzschicht an einem in den gleichformigen Flussigkeitsstrom eingetauchten geraden Kreiszylinder. *Dinglers Polytech. J.* 1911. 326: 321–324.

[4] Weidman, P. Impinging rotational stagnation-point flows. *International Journal of Non-Linear Mechanics*. 2017. 88: 97–101.

[5] Lok, Y. Y., Amin, N. and Pop, I. Non-orthogonal stagnation point flow towards a stretching sheet. *International Journal of Non-Linear Mechanics*. 2006. 41(4): 622–627.

[6] Labropulu, F. Unsteady stagnation-point flow of a viscoelastic fluid in the presence of a magnetic field. *International Journal of Mathematics and Mathematical Sciences*. 2008.

[7] Borrelli, A., Giantesio, G. and Patria, M.C. MHD orthogonal stagnation-point flow of a micropolar fluid with the magnetic field parallel to the velocity at infinity. *Applied Mathematics and Computation*. 2015. 264: 44–60.

[8] Hafidzuddin, E.H., Nazar, R., Arifin, N.M. and Pop, I. Effects of anisotropic slip on three-dimensional stagnation-point flow past a permeable moving surface. *European Journal of Mechanics-B/Fluids*. 2017. 65: 515–521.

[9] Rehman, F. U., Nadeem, S. and Haq, R. U. Heat transfer analysis for three-dimensional stagnation-point flow over an exponentially stretching surface. *Chinese Journal of Physics*. 2017. 55(4): 1552–1560.

[10] Mahapatra, T. R. and Sidui, S. Heat transfer in non-axisymmetric Homann stagnation-point flows towards a stretching sheet. *European Journal of Mechanics-B/Fluids*. 2017. 65: 522–529.

[11] Malashetty, M. S. and Swamy, M. S. Effect of gravity modulation on the onset of thermal convection in rotating fluid and porous layer. *Physics of Fluids*. 2011. 23(6): 64108.

[12] Sharidan, S., Amin, N. and Pop, I. g-jitter fully developed combined heat and mass transfer by mixed convection flow in a vertical channel. *International communications in heat and mass transfer*. 2005. 32(5): 657–665.

[13] Shafie, S., Amin, N. and Pop, I. g-Jitter free convection flow in the stagnation-point region of a three-dimensional body. *Mechanics Research Communications*. 2007. 34(2): 115–122.

[14] Babu, M. J. and Sandeep, N. Effect of nonlinear thermal radiation on non-aligned bio-convective stagnation point flow of a magnetic-nanofluid over a stretching sheet. *Alexandria Engineering Journal*. 2016. 55(3): 1931–1939.

[15] Gupta, S., Kumar, D. and Singh, J. MHD mixed convective stagnation point flow and heat transfer of an incompressible nanofluid over an inclined stretching sheet with chemical reaction and radiation. *International Journal of Heat and Mass Transfer*. 2018. 118: 378–387.

[16] Amirsom, N. A., Uddin, M. J. and Ismail, A. I. Three dimensional stagnation point flow of bionanofluid with variable transport properties. *Alexandria Engineering Journal*. 2016. 55(3): 1983–1993.

[17] Cebeci, T. and Bradshaw, P. *Finite-difference solution of boundary-layer equations. In Physical and Computational Aspects of Convective Heat Transfer*. Berlin, Heidelberg: Springer. 1984.

[18] Sharidan, S. *Mathematical Modelling of g-Jitter Induce Free Convection*. Universiti Teknologi Malaysia: Ph.D. Thesis. 2005.

[19] Tiwari, Raj Kamal, and Manab Kumar Das. Heat transfer augmentation in a two-sided lid-driven differentially heated square cavity utilizing nanofluids. *International Journal of Heat and Mass Transfer*. 2007. 50.9-10: 2002-2018.

[20] Rawi, N.A., Kasim, M., Rahman, A., Mat Isa, Z., Mangi, A. and Shafie, S. G-jitter effects on the mixed convection flow of nanofluid past an inclined stretching sheet. *Frontiers in Heat and Mass Transfer*. 2017. 8.